

RSC Advances



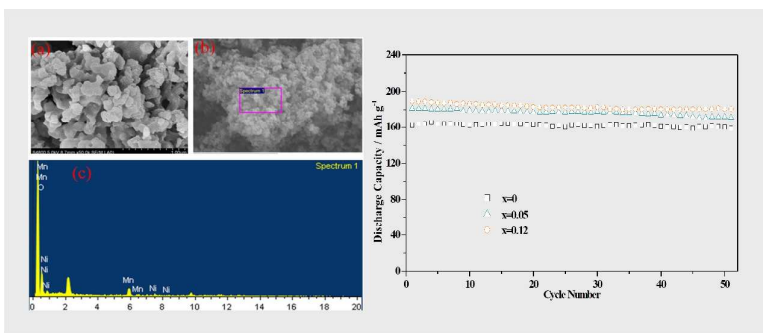
This is an *Accepted Manuscript*, which has been through the Royal Society of Chemistry peer review process and has been accepted for publication.

Accepted Manuscripts are published online shortly after acceptance, before technical editing, formatting and proof reading. Using this free service, authors can make their results available to the community, in citable form, before we publish the edited article. This *Accepted Manuscript* will be replaced by the edited, formatted and paginated article as soon as this is available.

You can find more information about *Accepted Manuscripts* in the [Information for Authors](#).

Please note that technical editing may introduce minor changes to the text and/or graphics, which may alter content. The journal's standard [Terms & Conditions](#) and the [Ethical guidelines](#) still apply. In no event shall the Royal Society of Chemistry be held responsible for any errors or omissions in this *Accepted Manuscript* or any consequences arising from the use of any information it contains.

Graphical Abstract



Text for Table of Contents

Cobalt doped to modify the structure of lithium-rich cathode and obtain the material with superior electrochemical performance.

ARTICLE

Cobalt-doped lithium-rich cathode with superior electrochemical performance for lithium-ion batteries

Cite this: DOI: 10.1039/x0xx00000x

Bing Yuan,^a Shi-Xuan Liao,^a Yan Xin,^b Yanjun Zhong,^a Xiaxing Shi,^a Longyan Li^a and Xiaodong Guo^{*a}

Received 00th January 2012,

Accepted 00th January 2012

DOI: 10.1039/x0xx00000x

www.rsc.org/

Li-rich Mn-based Co-doped $\text{Li}_{1.231}\text{Mn}_{0.615-0.75x}\text{Ni}_{0.154}\text{Co}_x\text{O}_2$ ($x=0, 0.02, 0.05, 0.07, 0.10, 0.12, 0.15, 0.20, 0.25$) cathode materials were prepared by a facile combustion method. X-Ray diffraction analysis indicates that the crystal structure of materials has been modified by the doped cobalt ions. The capacity differential results obtained from the galvanostatic charge/discharge process within 2.0 and 4.8 V (vs. Li/Li^+) indicate that the cobalt doped in the material could conduce to lithium ions re-embedded into the structure and increase the electrical properties. Compared with the electrochemical properties of these materials, the optimum doped sample is $\text{Li}_{1.231}\text{Mn}_{0.525}\text{Ni}_{0.154}\text{Co}_{0.12}\text{O}_2$ ($x=0.12$), which delivers an extremely minimum irreversible capacity of 59.1 mAh/g with the highest coulombic efficiency of 82.6% and its discharge specific capacity maintains 180.7 mAh/g at 1 C rate after 50 cycles.

1. Introduction

With the development of mobile electrical products, the demand for rechargeable batteries is rapidly growing. Lithium-ion batteries, which are made of environmentally friendly materials with high energy density and long cycle life, are widely used.¹ Since Numata et al.² reported the solid solution of the LiCoO_2 - Li_2MnO_3 system in 1997, Li_2MnO_3 -stabilized cathode has been widely investigated as an alternative to LiCoO_2 cathode in lithium-ion batteries for their high theoretical capacity (about 350 mAh/g) at higher voltages, lower cost and improved thermal stability.³⁻⁵

However, the poor electrochemical performances of this kind of materials obstruct severely their application. Nowadays several methods have been used by researchers to further improve the electrochemical properties of the cathode, such as preparing materials by the template method⁶, special nanostructures⁷, modifying the material surface with oxides (e.g., ZnO)⁸ or adding a conductive substances (e.g., carbon)⁹. However, these approaches are very complex and expensive. Tang et al.¹⁰ synthesized a series of $\text{Li}[\text{Li}_x\text{Mn}_{0.65(1-y)}\text{Ni}_{0.35(1-y)}\text{O}_2]$ materials by the conventional solid-state method, and found that the electrochemical performance of Co-doped materials was significantly improved relative to the pristine one. Their disappointing specific capacity still can't reach the application requirements, but this work indicates that the partially substituted manganese in LiMO_2 may be a simple effective method to improve significantly the electrochemical properties of the materials.

In the previous work⁴, the composite $\text{Li}_{1.231}\text{Mn}_{0.615}\text{Ni}_{0.154}\text{O}_2$ by a facile combustion synthesis has been prepared. On this basis, we herein report a series of Co-doped $\text{Li}_{1.231}\text{Mn}_{0.615-0.75x}\text{Ni}_{0.154}\text{Co}_x\text{O}_2$ ($x=0, 0.02, 0.05, 0.07, 0.10, 0.12, 0.15, 0.20,$

0.25) samples by this method. When $x=0.12$, the material shows the best performance, with a high discharge capacity of 180.7 mAh/g at 1 C (here, 1 C corresponds to 200 mA/g) rate after 50 cycles. In addition, we found that the cobalt doped in the material could conduce to lithium ions re-embedded into the structure and increase the electrical properties.

2. Experimental

2.1 Preparations

$\text{Li}_{1.231}\text{Mn}_{0.615-0.75x}\text{Ni}_{0.154}\text{Co}_x\text{O}_2$ ($x=0, 0.02, 0.05, 0.07, 0.10, 0.12, 0.15, 0.20, 0.25$) were prepared by a conventional facile combustion method using stoichiometric amounts of lithium salt (LiNO_3), manganese salt ($\text{Mn}(\text{CH}_3\text{COO})_2 \cdot 4\text{H}_2\text{O}$), nickel salt ($\text{Ni}(\text{CH}_3\text{COO})_2 \cdot 4\text{H}_2\text{O}$), and the cobalt salt ($\text{Co}(\text{NO}_3)_2 \cdot 6\text{H}_2\text{O}$) solution in deionized water. Meanwhile, we milled an appropriate amount of sucrose and stirred the solution under 90 °C to evaporate the most of water. After baking in oven at 120 °C for 3 hours, the chocolate-brown substance in the form of bread was obtained. Then the substance was ignited to obtain an ash-like precursor. Finally, the precursor was calcined in air at 500 °C for 5 hours, re-heated at 750 °C or 900 °C for 10 hours and then cooled naturally.

2.2 Characterizations

The crystalline phases of the prepared samples were identified using a Philips X-ray diffractometer PW 1730 with Cu-K α radiation. XRD data were collected at a scan speed of 0.06 °/s in the 2 θ range of 10 to 70 °. The electrochemical characterization was tested using the CR 2032 button battery. Active material ($\text{Li}_{1.231}\text{Mn}_{0.615-0.75x}\text{Ni}_{0.154}\text{Co}_x\text{O}_2$), acetylene black and polyvinylidene fluoride (PVDF) with the weight ratio of 80:10:10 were mixed by ball milling in N-methyl-2-pyrrolidone (NMP) solvent to obtain the homogeneous slurry. Then the cathode slurry was coated onto aluminum foils (about 40 μm) and dried at 100 °C for 12 h in vacuum.

The electrode was punched into discs of 14 mm in diameter. CR2032-type coin cells were assembled in an Argon atmosphere glove box (Universal 5641101, Dellix, Chengdu, China) with H₂O and O₂ contents below 1 ppm. Metallic lithium foil was used as the counter electrode. The electrolyte was 1 M LiPF₆ dissolved in a mixture of ethylene carbonate (EC) and dimethyl carbonate (DMC) (1:1, v/v) and Celgard 2400 polyethylene was used as the separator. The unit cell was typically cycled in a voltage range of 2.0-4.8 V vs. Li/Li⁺.

3. Results and discussion

Figure 1 shows the SEM image and EDS result of the non-doping precursor (x=0). SEM micrographs shown in Figure 1a, b reveal a fluffy porous morphology formed by small particles aggregated, which is a result of the decomposition of sucrose, nitrate, and acetate, accompanying the escaping gases such as CO₂ and H₂O.⁴ The EDS estimation of the selected region in SEM image of Figure 1b is depicted in Figure 1c. A molar ratio of Mn/Ni=4.01 accorded well with theoretical value is measured in the precursor, indicating the loss of transition metal ions could be effectively avoided through the facile combustion synthesis method.

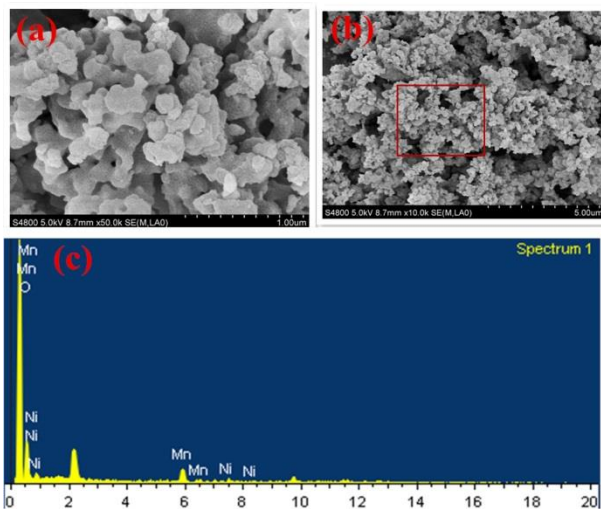


Figure 1. SEM micrograph (a) and (b) of x=0, EDS spectrum (c) of x=0.

Figure 2 illustrates the XRD patterns of the materials Li_{1.231}Mn_{0.615-0.75x}Ni_{0.154}Co_xO₂ prepared with different x values. All of the diffraction patterns can be identified as a layered oxide structure based on a hexagonal α -NaFeO₂ structure (space group: 166, *R3m*). The sharp and well-defined peaks suggest that the compounds are generally well crystallized. There are some weak peaks locating at 20° < 2θ < 25° which is marked with rectangle in Figure 2(I), and they cannot be indexed to *R3m* symmetry. It has been proven that they are consistent with the case of LiMn₆ cation ordering in the transition metal layers of Li₂MnO₃, which can be indexed to the monoclinic unit cell, C2/m.^{11,12} Moreover, with the increase of x values, the weak peaks between 21° and 25° become weaker, which attributes largely to the effective substitution of Co³⁺ for Mn⁴⁺ ions occurring in the hexagonal structures, and the variation of Co content may more or less modify the crystal structures.¹³⁻¹⁵ Figure 2(III) shows the peaks (018) and (110) between 64° and 66°. With the increase of cobalt content, the peaks move to the right side progressively and continuously, also indicating the

Co-doped well and the crystal structures have been modified. Overall reduced lattice parameters can be observed in the Co-doped samples, as summarized in Table 1.^{16,17}

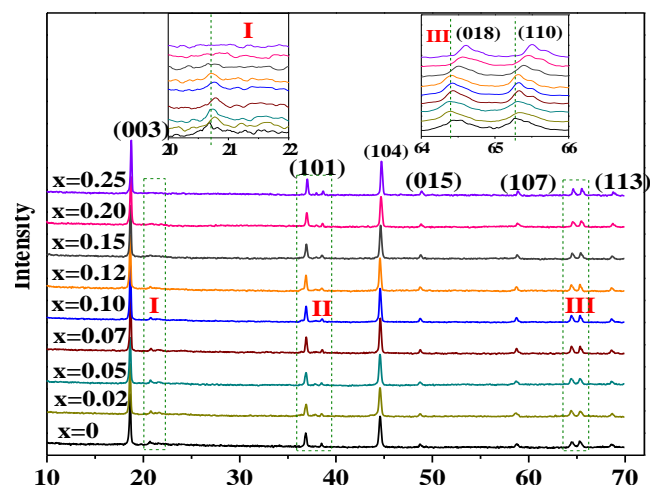


Figure 2. XRD patterns for Li_{1.231}Mn_{0.615-0.75x}Ni_{0.154}Co_xO₂ (x=0, 0.02, 0.05, 0.07, 0.10, 0.12, 0.15, 0.20, 0.25).

Table 1. Lattice parameters of the layered oxide compositions.

X	a (Å)	c (Å)	V (Å ³)
0.00	2.8633	14.2669	101.67
0.02	2.8531	14.2593	100.52
0.05	2.8545	14.2580	100.61
0.07	2.8538	14.2439	100.46
0.10	2.8547	14.2363	100.47
0.12	2.8544	14.2517	100.56
0.15	2.8521	14.2250	100.21
0.20	2.8499	14.2170	100.00
0.25	2.8477	14.2065	99.77

The most important advantage of yLi₂MnO₃(1-y)LiMO₂ is its high reversible capacity, but the prolapse of Li₂O during the initial cycle will lead to a high irreversible capacity loss and a low coulombic efficiency.¹⁸ Figure 3 compares the initial and the second charge/discharge details of the Li_{1.231}Mn_{0.615-0.75x}Ni_{0.154}Co_xO₂ (x=0, 0.02, 0.05, 0.07, 0.10, 0.12, 0.15, 0.20, 0.25) with current density of 20 mA/g (0.1 C) between 2.0 and 4.8 V at room temperature. As shown in Figure 3, the cobalt doped material has been significantly improved the initial discharge capacity, and reduced the irreversible capacity. It can also be seen in Figure 4, which depicts the irreversible capacity and the corresponding coulombic efficiency in the initial charge/discharge cycle of samples with different x values. When the x values are 0, 0.05, 0.12 and 0.25, the initial discharge specific capacities are 201.3, 240.8, 280.7 and 259.1 mAh/g, respectively, with the coulombic efficiency of 65.5%, 64.9%, 82.6% and 66.0%. The minimum irreversible capacity (59.1 mAh/g) and the maximum coulombic efficiency (82.6%) are achieved at the value of x=0.12.

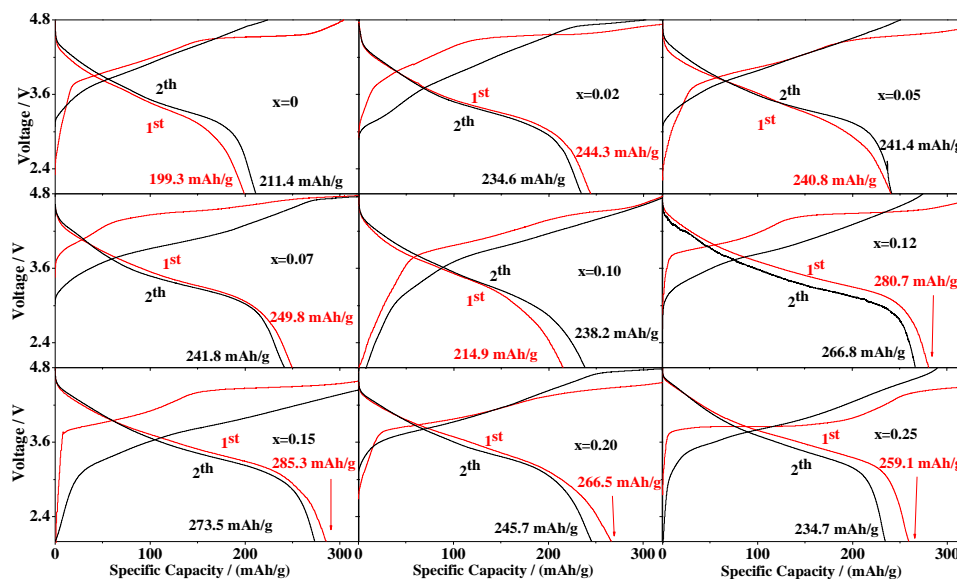


Figure 3. Voltage profiles for the first and second charge and discharge curves of $\text{Li}_{1.231}\text{Mn}_{0.615-0.75x}\text{Ni}_{0.154}\text{Co}_x\text{O}_2$ ($x=0, 0.02, 0.05, 0.07, 0.10, 0.12, 0.15, 0.20, 0.25$) between 2.0 and 4.8 V.

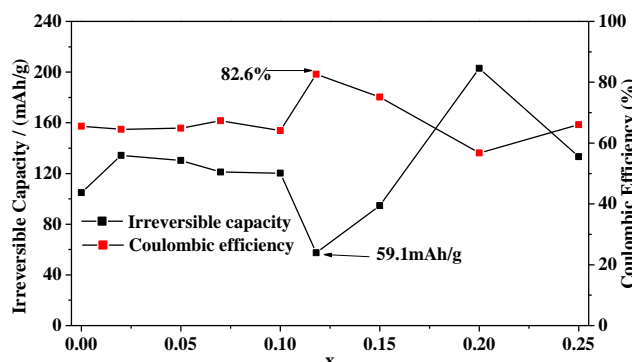


Figure 4. Initial charge and discharge irreversible capacity and coulombic efficiency of the materials $\text{Li}_{1.231}\text{Mn}_{0.615-0.75x}\text{Ni}_{0.154}\text{Co}_x\text{O}_2$ ($x=0.02, 0.05, 0.07, 0.12, 0.15, 0.20, 0.25$).

The rate performances of the samples measured between 0.1 C and 1 C are shown in Figure 5a. The details of the rate performances of the materials with different x values are listed in Table 2. When $x=0, 0.05$ and 0.12 , the retention ratios of 1 C (relative to 0.1 C) are 73.9%, 72.0% and 70.9%, respectively. It is obvious that when $x=0.05$ and 0.12 the electrode exhibits an excellent performance in all current rates, and delivers an average discharge capacity of 180.4 and 189.2 mAh/g at 1 C, respectively.

In order to get a deeper understand of the effect of cobalt content on oxidation/reduction during the charge/discharge process of the materials, the initial (20 mA/g) and the thirtieth (200 mA/g) charge/discharge differential capacity ($dQ/dV \sim V$) curves are shown in Figure 5b. According to the literature, the initial charge/discharge curves of $y\text{Li}_2\text{MnO}_3$ ($1-y$) LiMO_2 materials can be divided into four regions (regions A to D) as follows¹⁹: Li deintercalation with oxidation of M ion in LiMO_2 component (<4.4 V, region A), Li_2O extraction by oxidation of oxide ion in Li_2MnO_3 component (>4.4 V, region B, irreversible), Li insertion by reduction of M ion (>3.5 V,

region C) and Li insertion by reduction of Mn^{4+} ion (<3.5 V, region D).

The dQ/dV curves at different current density of 20 mA/g and 200 mA/g, corresponding to 1st and 30th cycle separately of aforementioned rate cycling process (Figure.5a) are shown in Figure 5b. Figure 5b (left) shows that the peak intensity of region A (about 3.9 V) increases with the increase of cobalt content. The result suggests that the replacement of cobalt to manganese makes a great change in the initial charge/discharge process, and more specifically, the doping of Co causes the variability of the initial charge specific capacity of LiMO_2 . In another sense, the results also show that Co has been successfully doped into the internal structure of materials. From the comparison of the region B and B' (about 3.4 V), we can find that the region B' is almost disappeared at 200 mA/g,

Table 2. Average discharge capacity of the samples for different rates.

X	Average Capacity (mAh/g)				Capacity Retention Ratio (%)
	0.1C	0.2C	0.5C	1C	
0.00	217.3	210.3	182.0	160.6	73.9
0.02	233.7	211.4	178.5	161.3	69.0
0.05	250.6	230.6	194.9	180.4	72.0
0.07	235.8	210.2	171.1	158.3	67.0
0.10	219.5	198.8	143.6	104.8	47.8
0.12	266.6	239.2	204.6	189.0	70.9
0.15	263.7	222.4	189.7	162.7	61.7
0.20	246.6	213.3	170.5	148.0	60.0
0.25	229.0	204.8	173.8	154.3	67.3

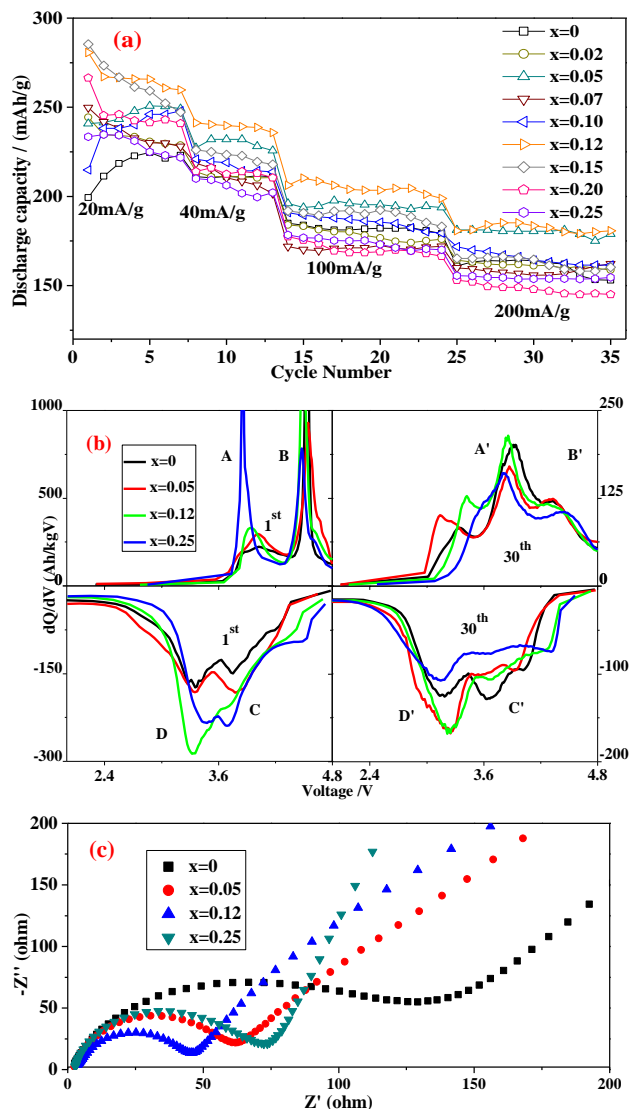


Figure 5. (a) Rate capacity of the samples, (b) Initial (20 mA/g) and the 30th (200 mA/g) charge/discharge differential capacity (dQ/dV -V) curves for different samples, (c) EIS plots of the samples with fresh coin cells.

which verifies the prolapse of Li2O is irreversible¹⁸. The peak intensity of region D (about 3.4V) changes with the cobalt content. It indicated the cobalt doped have modified the structure of the materials, which made more lithium ions re-embedded into the crystal in the discharge process. In the region D', at high rate, the stronger of intensity when $x = 0.05$ and $x=0.12$ means these two Co-doped composites possess better rate capabilities, illustrating the stable modified structures. The improved electrochemical properties are mainly due to the right amount of cobalt doping, which reduced the charge/discharge transfer resistance (R_{ct}) as demonstrated in Figure 5c. By comparing the diameter of the main semicircles, the $x=0.05$ and $x=0.12$ show relatively smaller R_{ct} value than those of non-doping ($x=0$) and high content Co doping ($x=0.25$) composites.

The practical application of reversible lithium-ion batteries requires an excellent cycling performance. The aforementioned two kinds of cobalt-doped materials ($x=0.05$ and 0.12) with excellent rate performances (Figure 5a) also demonstrate attractive cycling properties, as shown in Figure 6. They are

tested at 200 mA/g over 50 cycles after 10 cycles at current densities of 10, 40, 100 mA/g. Figure 6 shows all the three solid solutions, $\text{Li}_{1.231}\text{Mn}_{0.615-0.75x}\text{Ni}_{0.154}\text{Co}_x\text{O}_2$ ($x=0, 0.05, 0.12$), which show high retention efficiency values during the cycles. The sample with $x=0.12$ delivers the best performance, and the discharge capacity is 180.7 mAh/g at 1 C rate after 50 cycles, which means 95% of initial capacity is remained after the cycling process.

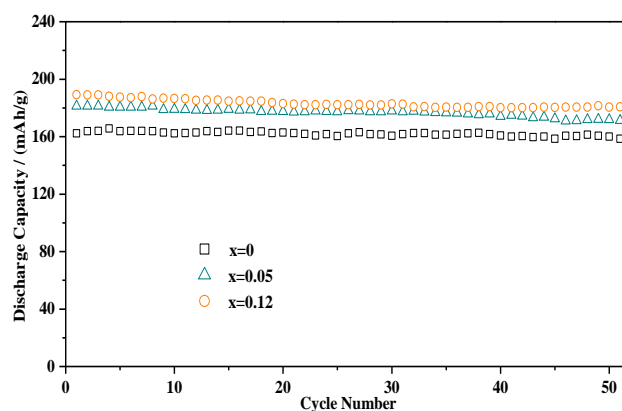


Figure 6. Cycling stability of materials $\text{Li}_{1.231}\text{Mn}_{0.615-0.75x}\text{Ni}_{0.154}\text{Co}_x\text{O}_2$ ($x=0, 0.05, 0.12$) electrodes measured at 1 C in the voltage range of 2.0 and 4.8 V.

Conclusions

A series of solid solutions $\text{Li}_{1.231}\text{Mn}_{0.615-0.75x}\text{Ni}_{0.154}\text{Co}_x\text{O}_2$ ($x=0, 0.02, 0.05, 0.07, 0.10, 0.12, 0.15, 0.20, 0.25$) have been successfully synthesized by an effective and facile combustion method. X-Ray diffraction analysis indicates that the crystal structure of materials have been modified by the doped cobalt ions. And it demonstrate from differential capacity curves and EIS plots that the structural change could conduce to lithium ions re-embedded into the structure and increase the electrical properties. Compared with the electrochemical properties in terms of initial irreversible capacity, initial coulombic efficiency, rate performance and long-cycle performance, the $x=0.12$ sample shows the best electrochemical performance with the minimum irreversible capacity of 59.1 mAh/g and the highest initial coulombic efficiency of 82.6%. Moreover, it has a high discharge capacity of 180.7 mAh/g after 50 cycles at 1 C rate, which means 95% of initial capacity is remained over the cycling test. In conclusion, we have modified the crystal structure of materials by cobalt ions doping, and the extra ordinary improved electrochemical performances are obtained when adopting appropriate doping contents. The optimum doped sample is $\text{Li}_{1.231}\text{Mn}_{0.525}\text{Ni}_{0.154}\text{Co}_{0.12}\text{O}_2$ ($x=0.12$).

Acknowledgements

This work was supported by the Sichuan University Funds for Young Scientists (grant number 2011SCU11081), the Research Fund for the Doctoral Program of Higher Education, and the Ministry of Education (grant number 20120181120103). The Analysis and Test Center of Sichuan University also supported this study.

Notes and references

- ^a College of Chemical Engineering, Sichuan University, Chengdu 610065, China.
- ^b Department of Chemical Engineering, Tsinghua University, Beijing 100084, China.
- * Corresponding author: Xiaodong Guo (Xiaodong2009@scu.edu.cn).
1. J.-M. Tarascon and M. Armand, *Nature*, 2001, **414**, 359-367.
 2. N. K., Y. S. and S. C., *SYNTHESIS OF SOLID SOLUTIONS IN A SYSTEM OF LiCOO₂-Li₂MNO₃ FOR CATHODE MATERIALS OF SECONDARY LITHIUM BATTERIES*, 1997.
 3. F. Wu, N. Li, Y. Su, H. Shou, L. Bao, W. Yang, L. Zhang, R. An and S. Chen, *Advanced Materials*, 2013, **25**, 3722-3726.
 4. S. X. Liao, B. H. Zhong, X. Guo, X. X. Shi and W. B. Hua, *European Journal of Inorganic Chemistry*, 2013, **2013**, 5436-5442.
 5. M. M. Thackeray, C. S. Johnson, J. T. Vaughey, N. Li and S. A. Hackney, *Journal of Materials Chemistry*, 2005, **15**, 2257-2267.
 6. S. Qiu, Z. Chen, F. Pei, F. Wu, Y. Wu, X. Ai, H. Yang and Y. Cao, *European Journal of Inorganic Chemistry*, 2013, **2013**, 2887-2892.
 7. J. Zhao and Y. Wang, *ECS Transactions*, 2014, **61**, 83-90.
 8. Y.-K. Sun, Y.-S. Lee, M. Yoshio and K. Amine, *Electrochemical and Solid-State Letters*, 2002, **5**, L1-L1.
 9. J. Kim, B. Kim, J.-G. Lee, J. Cho and B. Park, *Journal of power sources*, 2005, **139**, 289-294.
 10. Z. TANG, Z. WANG, X. LI and W. PENG, *Preparation and electrochemical properties of Co-doped and none-doped Li[Li_xMn_{0.65(1-x)}Ni_{0.35(1-x)}]O₂ cathode materials for lithium battery batteries*, Elsevier, Amsterdam, PAYS-BAS, 2012.
 11. J. Bréger, M. Jiang, N. Dupré, Y. S. Meng, Y. Shao-Horn, G. Ceder and C. P. Grey, *Journal of Solid State Chemistry*, 2005, **178**, 2575-2585.
 12. D. Luo, G. Li, X. Guan, C. Yu, J. Zheng, X. Zhang and L. Li, *Journal of Materials Chemistry A*, 2013, **1**, 1220-1227.
 13. F. Liu, S. Zhang, C. Deng, Q. Wu, M. Zhang, F. Meng, H. Gao and Y. Sun, *Journal of The Electrochemical Society*, 2012, **159**, A1591-A1597.
 14. C. Wang, S. Lu, S. Kan, J. Pang, W. Jin and X. Zhang, *Journal of Power Sources*, 2009, **189**, 607-610.
 15. H. Huang, C. Wang, W. Zhang, Y. Gan and L. Kang, *Journal of Power Sources*, 2008, **184**, 583-588.
 16. L. R. Bragg, 1987, pp. Longman [Imprint]; Pearson Education, Limited.
 17. A. V. Kolopakov and I. R. Prudnikov, *Moscow University Physics Bulletin*, 1991, **46**, 4-27.
 18. A. R. Armstrong, M. Holzapfel, P. Novák, C. S. Johnson, S.-H. Kang, M. M. Thackeray and P. G. Bruce, *Journal of the American Chemical Society*, 2006, **128**, 8694-8698.
 19. T. Arunkumar, Y. Wu and A. Manthiram, *Chemistry of materials*, 2007, **19**, 3067-3073.